Saudi Pharmaceutical Journal 32 (2024) 102066

HOSTED BY

Contents lists available at ScienceDirect

Saudi Pharmaceutical Journal

journal homepage: www.sciencedirect.com

Biocompatible gelatin-coated ferrite nanoparticles: A magnetic approach to advanced drug delivery

Varda Shakeel [a], Iftikhar Hussain Gul [a,*], Peter John [b], Attya Bhatti [b]

[a] Thermal Transport Laboratory, School of Chemical and Materials Engineering, National University of Sciences and Technology, Islamabad, Pakistan
[b] Atta-Ur-Rahman School of Applied Biosciences (ASAB), National University of Sciences and Technology (NUST), Islamabad, Pakistan

ARTICLE INFO

Keywords:
Magnetic nanoparticles
Drug delivery
Hemolysis
Biocompatibility
Cytotoxicity

ABSTRACT

Nanotechnology has transformed drug delivery, offering opportunities to enhance treatment outcomes while minimizing adverse effects. This study focuses on gelatin-coated cobalt and manganese ferrite nanoparticles for potential drug delivery applications. The synthesis involved a co-precipitation method, and the nanoparticles were characterized using various techniques, including X-ray diffraction (XRD), scanning electron microscopy (SEM), Fourier-transform infrared spectroscopy (FTIR), Raman spectroscopy, and vibrating sample magnetometer (VSM). Results revealed stable structures, distinct chemical features introduced by gelatin coating, and unique magnetic properties. The hemolysis assay demonstrated reduced hemolytic activity with gelatin coating, enhancing biocompatibility. Drug release studies indicated differential release profiles, with gelatin-coated cobalt ferrite exhibiting higher drug release compared to gelatin-coated manganese ferrite. The Higuchi model supported diffusion-controlled drug release for gelatin-coated cobalt ferrite. These findings suggest the potential of gelatin-coated ferrite nanoparticles for controlled and targeted drug delivery, highlighting their significance in advancing nanomedicine.

1. Introduction

Nanotechnology has recently revolutionized medicine delivery, providing new chances to improve treatment results and reduce adverse effects (Chandrasekaran et al., 2018). Magnetic nanoparticles (MNPs) are being developed as drug carriers among the wide variety of NPs used in biomedicine because of their logical magnetic features. They may be guided by an external magnetic field and release medications at cells thanks to magnetic properties. As a result, they can circumvent the drawbacks of traditional treatments and lessen a variety of unwanted effects (Kiani et al., 2022). Because of the diversity in the chemical composition, which results in a broad range of physical qualities in a number of applications, spinel ferrite is the most alluring category of iron oxide materials (Alfareed et al., 2022). When subjected to an alternating magnetic field, magnetic nanoparticles generate heat as the spinning magnetic moment relaxes (Khizar et al., 2020).

Additionally, magnetic nanoparticles have been used in magnetic resonance imaging (MRI) as enhanced contrast agents. Every time a new nanomaterial intended for biomedical uses was developed, its biosafety needed to be thoroughly investigated (Andrade et al., 2020). Due to their distinct magnetic and chemical characteristics, cobalt ferrite ($CoFe_2O_4$) and manganese ferrite ($MnFe_2O_4$) nanoparticles have emerged as viable candidates among the several nanomaterials explored for drug delivery (Kumar et al., 2022; Singh et al., 2010). Researchers have investigated covering these nanoparticles with gelatin, a biocompatible and adaptable biopolymer, to further optimize drug delivery systems (Park et al., 2021; Siddique and Chow, 2020; Topoisomerase II). The combination of these nanomaterials has the power to revolutionize biological applications by enabling targeted and regulated medication release (Reddy, 2019; Sagar, 2011; Albino et al., 2020).

$CoFe_2O_4$ are employed as heat agents, bio separation agents, and drug delivery agents to improve the signal response in MRI (Finetti et al., 2016). $CoFe_2O_4$ nanoparticles display outstanding stability in aqueous dispersion at physiological pH without varying in zeta potential or hydrodynamic size. $CoFe_2O_4$ is beneficial in a variety of biological and technical applications due to the precise control of its structure and composition (Parhizkar et al., 2019). As manganese ferrites have proven useful for many magnetic applications, including recording media devices, drug delivery, ferrofluid biosensors, and contrast-enhancers for magnetic resonance imaging (MRI) technology (Sahoo et al., 2014). Manganese ferrite ($MnFe_2O_4$) nanoparticles are regarded as an important class of spinel ferrites. Due to their high magnetic susceptibility,

* Corresponding author.
E-mail address: iftikhar.gul@scme.nust.edu.pk (I. Hussain Gul).

https://doi.org/10.1016/j.jsps.2024.102066
Received 8 January 2024; Accepted 7 April 2024
Available online 9 April 2024

manganese ferrite nanoparticles can be used in MRI as an ultrasensitive negative contrast agent for medication targeting. Additionally, these NPs frequently exhibit good biocompatibility and only mild toxicity when tested on HeLa cell lines (Akhlaghi and Najafpour-Darzi, 2021; Al-Rawi et al., 2020).

Gelatin-coated spinel ferrite nanoparticles have shown promise in drug delivery investigations in the past. Ansari et al., for example, created gelatin-coated cobalt ferrite nanoparticles for regulated drug delivery and effectively demonstrated their potential drug-loading and release behaviors (Ayyanaar et al., 2020; Majeed et al., 2021). Lakshmi and Geetha also reported on gelatin-coated magnetic nanoparticles for pH-responsive drug delivery, suggesting their ability to get through biological barriers (Wang et al., 2018). It is necessary to embed MNPs in non-toxic and biocompatible materials (matrix), such as polymer, calcium phosphate, silica, etc., or modify their surface with suitable coatings in order to meet the most important requirements for MNPs' use in various biomedical applications: biocompatibility and nontoxicity (Keshri and Biswas, 2022). Gelatin is also an extracellular matrix protein, which enables its use in gene transfection, medication administration, and wound dressings. Although it exhibits poor stability in aqueous solutions, it offers desirable qualities like natural origin, low cost, low toxicity, biodegradability, and non-immunogenicity (Dumontel et al., 2023).

In order to obtain focused and effective distribution, researchers have also looked at a variety of medications enclosed within gelatin-coated ferrite nanoparticles. With increased therapeutic effectiveness, Jain et al. examined the creation and optimization of gelatin-coated cobalt ferrite nanoparticles for the controlled release of anticancer drugs (Das et al., 2022). Similar research was conducted by Vandervoort et al., who investigated magnetically sensitive gelatin-coated manganese ferrite nanoparticles as prospective delivery systems for anticancer drugs (Shende and Pathan, 2021; Vandervoort and Ludwig, 2004).

In this research, we used gelatin-coated cobalt and manganese ferrite nanoparticles to further our understanding of drug conveyance applications. The creation of these nanocarriers, the characterization of their physicochemical characteristics, and the evaluation of their drug-loading potential and release kinetics will be the main objectives of our study. Our research introduces several novel aspects. Firstly, we explore the use of gelatin-coated ferrite nanoparticles for advanced drug delivery, leveraging the unique properties of these nanoparticles to enhance therapeutic efficacy while minimizing side effects. Additionally, we investigate the impact of gelatin coating on the structural and functional properties of the nanoparticles, providing valuable insights into their biocompatibility and potential applications in biomedicine.

2. Methodology

2.1. Synthesis of cobalt ferrite and manganese ferrite nanoparticles

High-purity reagents, including Fe $(NO_3)_2{\cdot}9H_2O$, Mn $(NO_3)_2{\cdot}6H_2O$, Co $(NO_3)_2{\cdot}6H_2O$, and NaOH (all from Sigma Aldrich), were meticulously employed in accordance with their stoichiometric proportions for the synthesis of $MnFe_2O_4$ and $CoFe_2O_4$ nanoparticles. Notably, gelatin polymers were chosen for their suitability as nanoparticle coatings, while acetic acid served as an effective dispersive medium for the subsequent nanocomposite formation. The choice of Ciprofloxacin as the drug for loading experiments added a pharmaceutical dimension to the study.

The co-precipitation method was meticulously implemented to prepare the divalent metal cations magnetic nanoparticles ($MnFe_2O_4$ and $CoFe_2O_4$). The process involved dissolving 16.00 g Fe $(NO_3)_3{\cdot}9H_2O$, 5.50 g Mn $(NO_3)_2{\cdot}4H_2O$, and 5.82 g Co $(NO_3)_2{\cdot}6H_2O$ in 200 ml deionized water to create an aqueous precursor solution. Sodium hydroxide was judiciously added dropwise to the solution while maintaining vigorous stirring, ultimately achieving a pH of 13. The reaction was carried out at a constant temperature of 80 °C for 1 h. Subsequent to cooling, the magnetic nanoparticles underwent multiple washing steps with deionized water and ethanol through centrifugation. Finally, the particles were sintered at 800 °C for 3 h, preparing them for advanced analysis (see Fig. 1).

2.2. Gelatin coated manganese and cobalt ferrite nanoparticles

An intricate and controlled approach was implemented for the synthesis of composite materials, incorporating manganese ferrite ($MnFe_2O_4$) and cobalt ferrite ($CoFe_2O_4$) nanoparticles embedded within a polymer matrix. The individual dispersion of 20 mg of each ferrite type in 10 ml of distilled water, facilitated by ultrasonic agitation for 20 min, was complemented by the dispersion of 10 mg of polymer particles in 20 ml of acetic acid using a magnetic mixer. This process was diligently repeated for both $MnFe_2O_4$ and $CoFe_2O_4$ ferrite types.

Post-dispersion, the polymer-acetic acid solution was carefully introduced into the ferrite dispersions after a 20-minute ultrasonication period. Subsequently, the combined solutions underwent an extended ultrasonication treatment for one hour, ensuring a comprehensive integration of the polymer and ferrite nanoparticles, thereby fostering effective material compatibility and distribution. Multiple rounds of washing were meticulously performed to stabilize the pH of the resulting composite solutions. The final composite products were then subjected to a careful drying process for approximately 2 h, facilitating the evaporation of solvents and yielding a well-defined composite structure (see Fig. 2).

2.3. Ciprofloxacin loaded gelatin coated manganese and cobalt ferrite nanoparticles

For the drug loading experiments, 0.0016 g of Ciprofloxacin was precisely diluted in 20 ml of methanol. This solution was then combined with 0.04 mg of nanocomposites in two separate beakers. The resulting mixture underwent stirring at room temperature for 24 h to ensure optimal drug loading. Following this, centrifugation was conducted at 6000 RPM for approximately 12 min to collect the drug-loaded particles for further detailed analysis.

The in-vitro release profile was studied in phosphate-buffered saline at various pH levels. To determine release kinetics, the released Ciprofloxacin was separated at different time intervals and quantified using UV spectroscopy. The impact of the gelatin coating on release was evaluated by comparing the release profile with a sonicated nanoparticle suspension. The data will be analyzed using mathematical models to understand the mechanism by which Ciprofloxacin is released from the nanoparticles (see Fig. 3).

2.4. Hemolysis assay

To assess potential blood cell toxicity, the hemolytic potential of bare and gelatin-coated cobalt ferrite ($CoFe_2O_4$) and manganese ferrite ($MnFe_2O_4$) nanoparticles was evaluated using a red blood cell (RBC) hemolysis assay. Blood was collected and centrifuged to isolate RBCs. After washing, RBCs were diluted in PBS. Test mixtures containing RBCs and each nanoparticle type (bare and coated versions of $CoFe_2O_4$ and $MnFe_2O_4$) were prepared alongside positive (deionized water for 100 % hemolysis) and negative controls (RBCs in PBS for 0 % hemolysis). Following incubation and centrifugation, the absorbance of the supernatant at 370 nm was measured using a UV–Vis spectrometer. The percentage of hemolysis was calculated for each sample. This experiment was performed in triplicate and data analysis will determine if there are significant differences in hemolytic potential between the bare and gelatin-coated nanoparticles.

3. Characterization techniques

The materials, namely $CoFe_2O_4$, $MnFe_2O_4$, $GCoFe_2O_4$, and

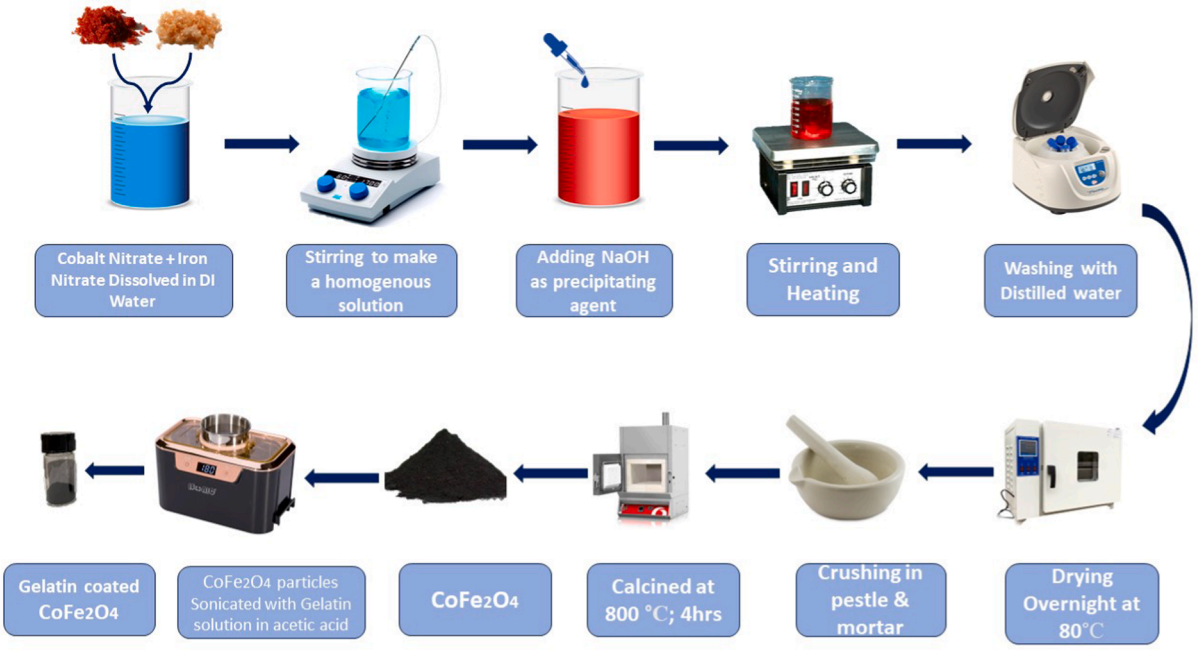

Fig. 1. Synthesis of spinel ferrites via co precipitation method.

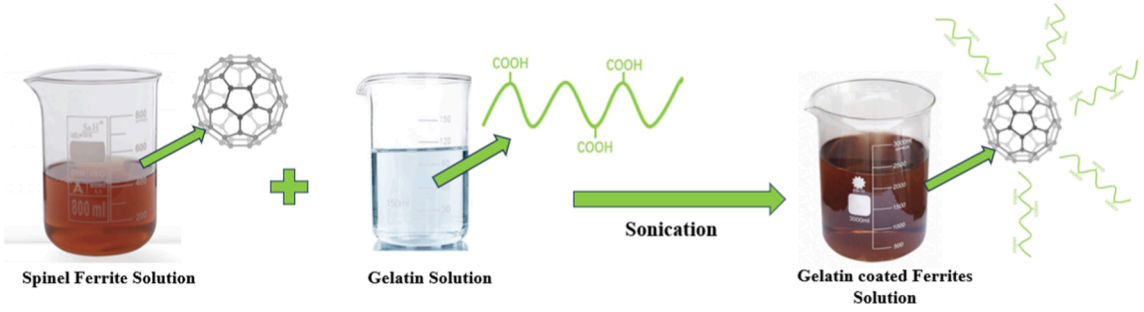

Fig. 2. Synthesis of gelatin coated spinel ferrites via Sonication.

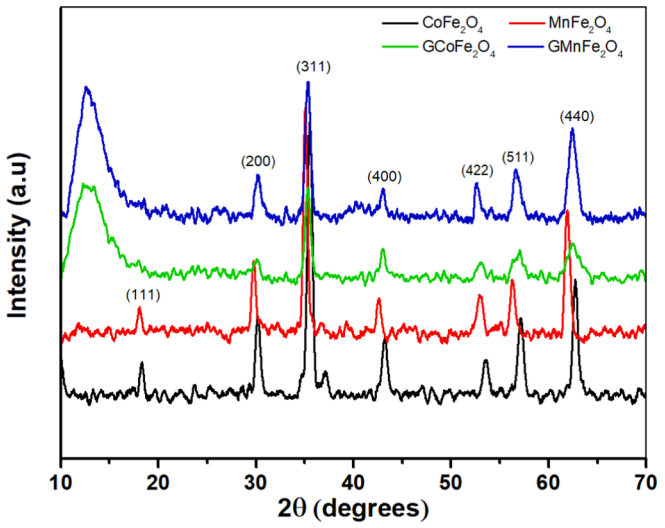

Fig. 3. The X-Ray diffraction Pattern of Bare and Gelatin coated $CoFe_2O_4$ and $MnFe_2O_4$ Nanocomposites.

$GMnFe_2O_4$, underwent comprehensive characterization using a suite of advanced techniques. X-Ray diffraction (XRD-6000, Shimadzu Co., Japan) utilizing CuKα radiation was employed at room temperature within the 10–80 two-theta range. Scanning Electron Microscope (HR-TEM) analysis using JEOL – JEM 2100 facilitated the determination of particle size. Fourier-transform infrared spectroscopy (FTIR) spanning 4000–400 cm^{-1} was utilized to analyze functional groups in the material, while Raman analysis provided further validation of vibrational modes and functional groups. Additionally, VSM analysis was conducted to elucidate the magnetic properties of the materials.

4. Results

4.1. XRD

An in-depth analysis of the X-ray diffraction (XRD) spectra of four samples, comprising both pure and gelatin-coated $CoFe_2O_4$ and $MnFe_2O_4$ nanoparticles was conducted to study their structural properties and potential implications for drug delivery applications. The XRD spectra exhibited characteristic peaks corresponding to the cubic spinel structure, including (111), (200), (311), (422), and (440) peaks, which were observed in all samples. Notably, the (311) and (422) peaks were more intense in $CoFe_2O_4$, suggesting that its particles possess smaller crystallite sizes compared to $MnFe_2O_4$ (see Fig. 3).

A significant disparity between the pure and coated samples was the

emergence of a broad peak at 2θ = 10°–20° in the gelatin-coated samples, attributed to the amorphous nature of the gelatin coating (Naghash-Hamed et al., 2022). Although the presence of the gelatin coating did not affect the characteristic peaks representing the cubic spinel structure, the broadening and reduced intensity of these peaks indicated the influence of the gelatin on the crystal lattice (Balatskiy et al., 2023). Additionally, upon calculating the crystallite size using the Scherrer equation, we observed that the gelatin-coated samples exhibited slightly larger crystallite sizes compared to the pure samples, indicating that the gelatin coating likely helps stabilize the particles and prevent excessive particle shrinkage (Vishwaroop and Mathad, 2020) (See Table 1).

These findings hold implications for drug delivery applications. The consistent lattice constant between pure and coated materials suggests that the gelatin coating does not significantly alter the material's properties, which is crucial to maintain drug integrity (Mushtaq et al., 2022). Furthermore, the biocompatible and biodegradable nature of the gelatin coating makes it an attractive candidate for various biomedical applications. Additionally, the gelatin coating's ability to control drug release rates offers potential for tailored drug delivery systems (Kulkarni and Mathad, 2018). Overall, our comprehensive XRD analysis underscores the promise of gelatin-coated $CoFe_2O_4$ and $MnFe_2O_4$ nanoparticles as viable candidates for targeted drug delivery applications, where the coating demonstrates favorable properties without compromising the underlying material's structural integrity. Moreover, the coating's role as a strain relaxer presents further opportunities for exploration in diverse biomedical settings (Battogtokh et al., 2022).

In this study, we calculated the crystallite size and lattice constant using the Scherrer equation and Bragg equation, respectively (Hashmi et al., 2023). The Scherrer equation allowed us to determine the crystallite size based on the width of the XRD peaks, and it is expressed as:

$$D = K\lambda / (\beta \cos\theta) \quad \text{(i)}$$

where D is the crystallite size, K is the Scherrer constant, λ is the X-ray wavelength, β is the full width at half maximum of the peak, and θ is the Bragg angle.

The Bragg equation, on the other hand, enabled us to calculate the d-spacing of the XRD peaks and is represented as:

$$d = \lambda / (2\sin\theta) \quad \text{(ii)}$$

where d is the d-spacing, λ is the X-ray wavelength, and θ is the Bragg angle.

These calculations revealed that the gelatin-coated samples exhibited slightly larger crystallite sizes and comparable lattice constants to the pure samples, highlighting the coating's effect on particle growth while preserving the material's underlying crystal structure (Dixit et al., 2022). The strain, an important parameter affecting material properties, was also assessed through the observed d-spacing and the known lattice constant for $CoFe_2O_4$ and $MnFe_2O_4$. The results indicated that the gelatin coating acted as a good strain relaxer, further emphasizing its potential significance in biomedical applications (Ma et al., 2022). These findings contribute valuable insights to the understanding of the structural properties of gelatin-coated nanoparticles and their relevance in drug delivery systems (Parikh and Parekh, 2015). The strain, a crucial parameter affecting material properties, was also evaluated through the observed d-spacing and the known lattice constant for $CoFe_2O_4$ and $MnFe_2O_4$. This comprehensive XRD analysis underscores the potential of gelatin-coated $CoFe_2O_4$ and $MnFe_2O_4$ nanoparticles as viable candidates for targeted drug delivery applications (Kulkarni and Mathad, 2019; Yattinahalli et al., 2013).

4.2. SEM

The FE-SEM analysis was used to regulate the morphology and average size of the $CoFe_2O_4$ and $MnFe_2O_4$ NPs. Spherical nanometric particles of cobalt ferrites could be observed in both samples. A slight particle agglomeration is suggestive of dipole dipole interaction between the nanoparticles (Parray et al., 2023). The average particle sizes obtained were 20–30 nm, approximately.

The images are all at the same magnification of 500,000× and have a scale bar of 0.5 μm. The images were taken at 20 kV, which is the voltage applied to the electron beam in the microscope. Scanning electron microscopy (SEM) provides estimations of the information regarding the surface morphology, shape, and size of grains. Synthesized ferrites had well-crystalline grains, according to SEM pictures. Both particle size and morphology were significantly impacted by the replacement of cations. The SEM micrograph shows the precise geometry of the grain size (See Fig. 4). When the resolution is raised, the buildup is also visible in the most recent sample (Junaid et al., 2022). Intergranular porosity and variations in grain size distribution can be seen in SEM pictures (Parray et al., 2023).

4.3. FTIR

In this research, we conducted Fourier-transform infrared (FTIR) spectroscopy analysis on four samples, including both pure and gelatin-coated specimens, to elucidate the influence of the gelatin coating on their chemical composition (See Fig. 6). The FTIR spectra revealed a prominent peak at 3417 cm^{-1} in all four samples, corresponding to the O—H bond stretching vibration of water. This peak was attributed to the aqueous solution in which all the samples were prepared (Hublikar et al., 2023). Bands within the 400–800 cm^{-1} region were identified as significant indicators of a spinel cubic structure upon revisiting the data. This observation underscores the complexity of the samples and enriches the analysis by providing insights into their structural characteristics. A striking disparity between the pure and coated samples was observed in the appearance of a peak at 1500 cm^{-1} in the coated samples, signifying the stretching vibration of the C—O bond in the gelatin coating. The absence of this peak in the pure samples further confirmed that it was a distinct characteristic of the gelatin coating (See Fig. 5).

In addition to the observations mentioned, further insights into the chemical composition were gleaned from the FTIR spectra, particularly regarding the vibrations of the Fe—O and Co—O bonds. The presence of these bonds is significant, especially in materials with spinel cubic structures, as they often involve transition metal ions such as iron (Fe) and cobalt (Co) coordinated with oxygen (O) atoms. The presence of the gelatin coating imparted notable effects on other peaks in the FTIR spectra as well. For instance, the peak at 2925 cm^{-1} in the coated samples exhibited slight broadening compared to the pure samples, attributed to the absorption of infrared radiation by the gelatin coating. Overall, the FTIR spectra of the coated samples were more intricate, owing to the introduction of new chemical bonds from the gelatin coating, each exhibiting distinct wavenumbers (See Table 2).

Table 1
Crystallographic Properties of $CoFe_2O_4$ and $MnFe_2O_4$, and Gelatin-Coated $CoFe_2O_4$ and $MnFe_2O_4$ Nanoparticles.

Sample	Crystallite Size (nm)	FCC Crystal Structure	Lattice Constant (Å)	Strain (%)
$CoFe_2O_4$	32	Yes	8.36	0.01
$MnFe_2O_4$	36	Yes	8.41	0.02
G-$CoFe_2O_4$	35	Yes	8.36	0.01
G-$MnFe_2O_4$	39	Yes	8.41	0.02

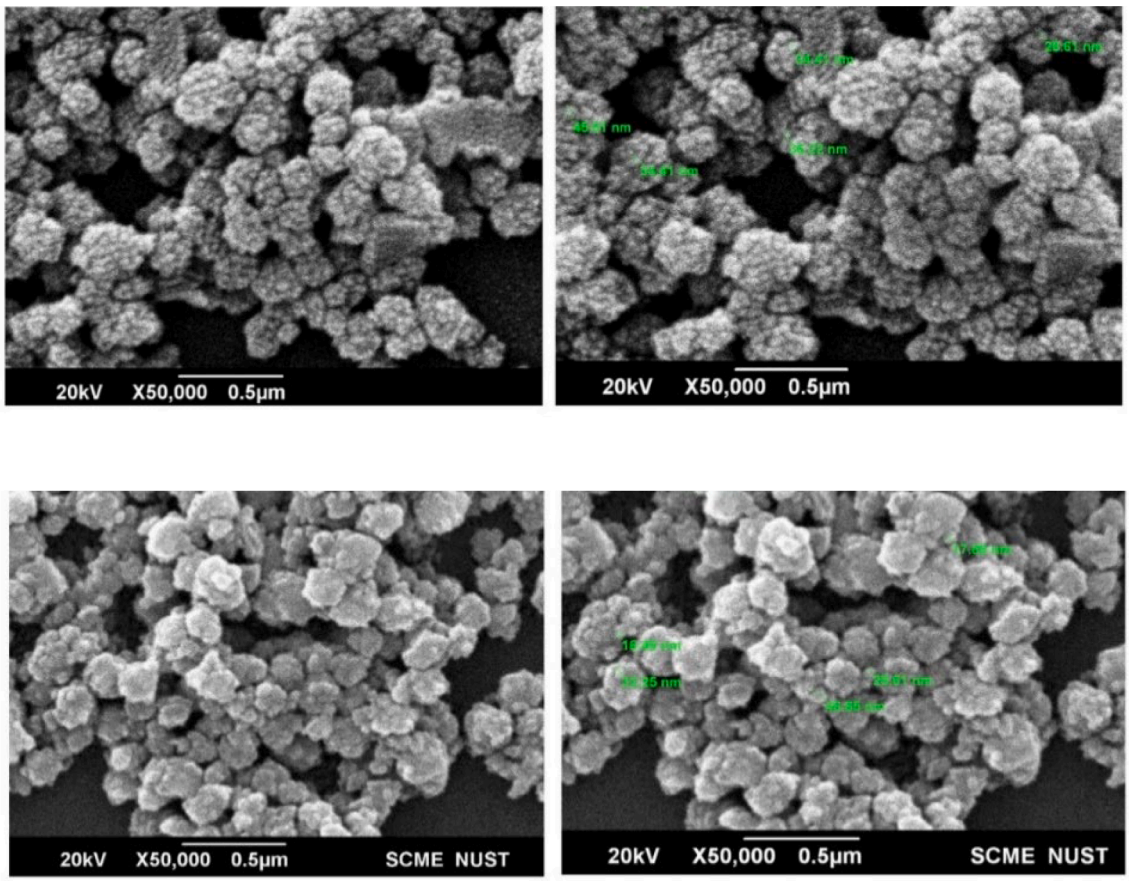

Fig. 4. SEM images of (a) $CoFe_2O_4$ and (b) $MnFe_2O_4$ Nanoparticles.

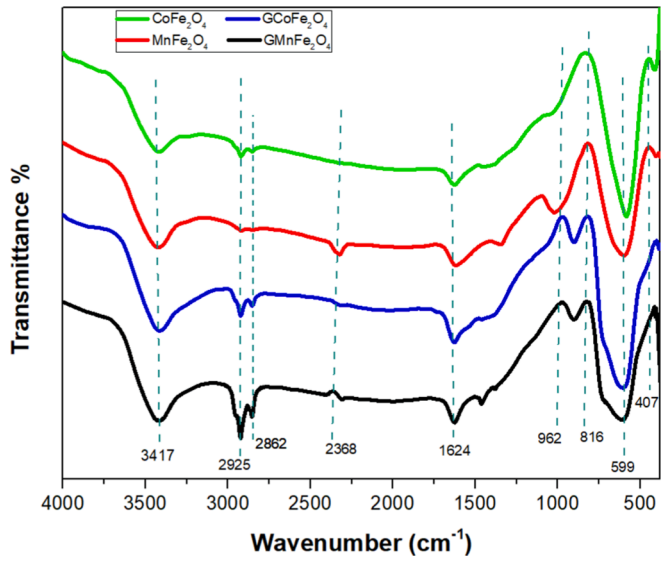

Fig. 5. The FTIR Spectra of Bare and Gelatin coated $CoFe_2O_4$ and $MnFe_2O_4$ Nanocomposites.

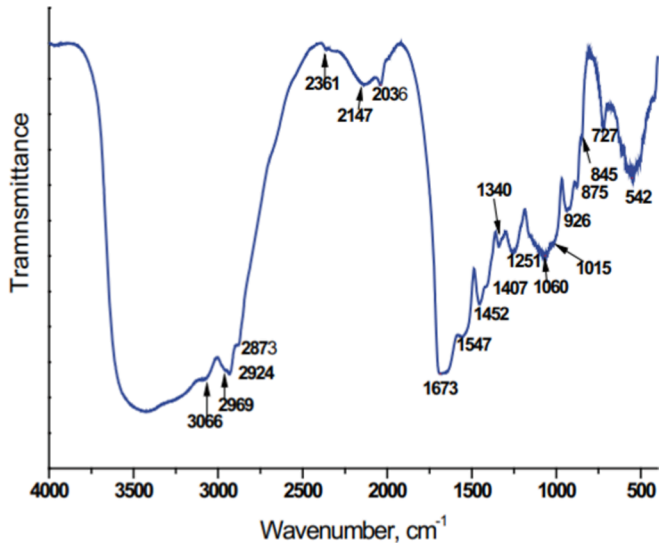

Fig. 6. The FTIR OF Pure Gelatin.

The implications of this study extend to drug delivery applications, as FTIR data has previously been employed in similar studies to investigate drug-gelatin interactions. In one notable study, FTIR analysis was utilized to study the interactions between the drug paclitaxel and a gelatin coating. The data revealed the formation of a protective layer around the drug, preventing its degradation and enhancing the stability of paclitaxel—an essential drug used in cancer treatment (Battogtokh et al., 2022). Similarly, in another study, FTIR data was employed to study the controlled release of the drug insulin from a gelatin coating. The results demonstrated that the gelatin coating dissolved at a specific rate, effectively controlling the release rate of insulin, which is crucial for diabetic patients. These findings emphasize the potential of gelatin-coated materials as promising carriers for controlled and targeted drug delivery, presenting opportunities for advancing pharmaceutical applications (Bahoor et al., 2023; Parikh and Parekh, 2015).

Table 2
Symmetric vibrations observed in FTIR Spectra of $CoFe_2O_4$ and $MnFe_2O_4$, and Gelatin-Coated $CoFe_2O_4$ and $MnFe_2O_4$ Nanoparticles.

Bond Vibration	Wavenumber Range (cm^{-1})	Description
Metal-Oxygen Stretching (Spinel)	400–800	Stretching of metal–oxygen bonds within the spinel crystal structure
Metal-Oxygen Stretching (Octahedral)	Around 600	Stretching of metal–oxygen bonds in octahedral sites
Metal-Oxygen Stretching (Tetrahedral)	Around 400	Stretching of metal–oxygen bonds in tetrahedral sites (may be weaker)

4.4. Raman spectroscopy

The Raman spectra of four distinct samples, namely pure $CoFe_2O_4$, $MnFe_2O_4$, G-$CoFe_2O_4$, and G-$MnFe_2O_4$ nanoparticles, were thoroughly analyzed. This analysis aimed to delve into their structural properties and evaluate their potential for drug delivery applications.

The Raman spectra of these samples exhibited characteristic peaks, particularly the tetrahedral breathing modes, which are indicative of the crystal structures of the materials. This is consistent with the findings of Gingasu et al. (2023). In the case of $CoFe_2O_4$, two distinct peaks were observed at 684 and 633 cm^{-1}. These peaks correspond to the tetrahedral breathing modes of A1g (1) and A1g (2), respectively. Similarly, Mn Fe_2O_4 exhibited a peak at 622 cm^{-1}, which is associated with the symmetric stretching of the Mn—O bond in the tetrahedral site (Gingasu et al., 2023).

Interestingly, the gelatin-coated samples, G-Co Fe_2O_4 and G-Mn Fe_2O_4, showed similar Raman peaks to their respective pure counterparts. However, the intensity of the A1g (1) peak was slightly lower in the coated samples (See Fig. 7). This phenomenon can be attributed to the gelatin coating absorbing some of the Raman light, thereby reducing the intensity of the A1g (1) peak in the coated samples (Carregal-Romero et al., 2022). This phenomenon can be attributed to the gelatin coating absorbing some of the Raman light, thereby reducing the intensity of the A1g (1) peak in the coated samples (Santos et al., 2022).

It is noteworthy that the gelatin coating did not significantly affect the other Raman peaks related to the vibrations of the Fe—O and Co—O bonds, as these peaks remained consistent with the expected Raman spectra of $CoFe_2O_4$, $MnFe_2O_4$, G-$CoFe_2O_4$, and G-$MnFe_2O_4$. Overall, these findings suggest that the gelatin coating does not substantially alter the structural properties of the materials, making them viable candidates for drug delivery applications (Mohammadi et al., 2022).

The Raman spectroscopy results offer promising prospects for drug delivery system design. By understanding the characteristic Raman spectra of different components within a drug delivery system, it is possible to optimize the system's design, ensuring precise drug release rates and stability (See Table 3). For instance, drug delivery systems could be designed to release drugs upon excitation of the tetrahedral breathing modes of the materials, potentially using a laser tuned to the Raman shift of these modes (Mohammadi et al., 2022).

The Raman spectra of ferric cobalt coated ferrite (FCCF) and bare cobalt ferrite (CF) were compared in the work by Nahar (2022). The A1g mode showed symmetric stretching of the oxygen anion, whereas the Eg mode suggested symmetric bending and the F2g mode related to

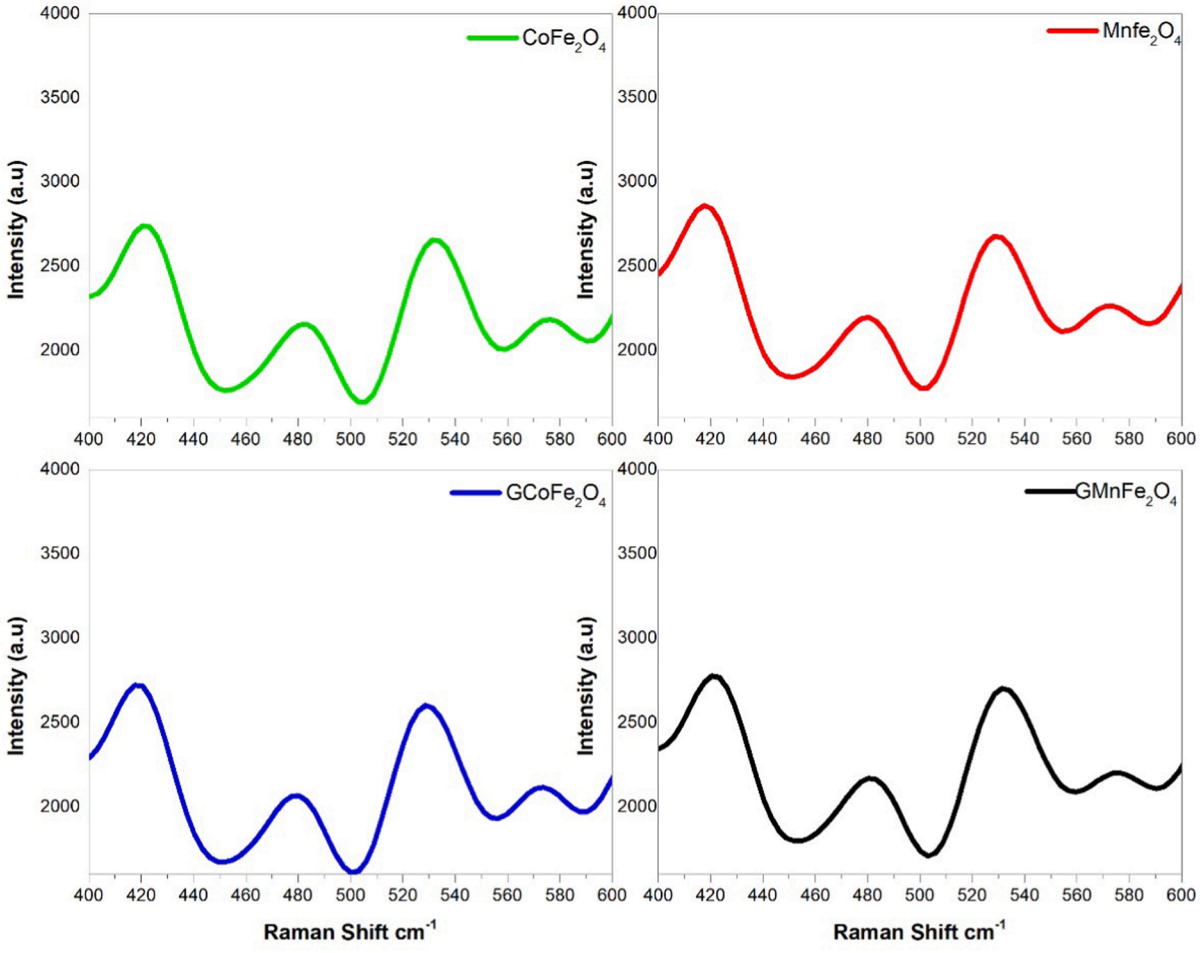

Fig. 7. The Raman Spectra of Bare and Gelatin coated $CoFe_2O_4$ and $MnFe_2O_4$ Nanocomposites.

Table 3
Symmetric vibrations observed in Raman Spectra of $CoFe_2O_4$ and $MnFe_2O_4$, and Gelatin-Coated $CoFe_2O_4$ and $MnFe_2O_4$ Nanoparticles.

Wavenumber Range (cm^{-1})	Vibration Mode	Description
~400	A_1g	Stretching mode of the metal–oxygen bonds at tetrahedral sites
~600	Eg	Bending mode of the metal–oxygen bonds at tetrahedral sites
~650	T_2g	Stretching mode of the metal–oxygen bonds at octahedral sites

asymmetric stretching of the oxygen anion in tetrahedral and octahedral sites. The lower frequency Raman modes (F2g and Eg) related to vibrations of the Fe—O bonds in octahedral sites. The FCCF Raman spectra revealed peak shifts compared to the bare CF, suggesting the existence of coating, possibly due to the strong absorption of Ferric Cobalt (FC). These findings reveal the structural changes generated by the FC coating on Cobalt Ferrite and highlight its potential uses (Nahar, 2022).

4.5. Vibrating sample magnetometer (VSM)

A thorough investigation of the magnetic properties and coercivity of cobalt ferrite ($CoFe_2O_4$) and manganese ferrite ($MnFe_2O_4$) samples, both uncoated and coated with gelatin, was conducted. The study utilized VSM spectra analysis to determine crucial parameters such as saturation magnetization (Ms), remanent magnetization (Mr), and coercivity (Hc). The results revealed that cobalt ferrite, known as a hard magnetic material, exhibited a pronounced and sharp magnetization curve with elevated Ms and Hc values, indicating its strong resistance to demagnetization even in the absence of an external magnetic field. On the contrary, manganese ferrite, characterized as a soft magnetic material, demonstrated lower Ms and Hc values, indicating its propensity to lose magnetization upon removal of the external magnetic field (See Fig. 8). Additionally, it was observed that the presence of a gelatin coating caused a slight reduction in the saturation magnetization and coercivity of cobalt ferrite. These findings hold significance in drug delivery applications, where magnetic nanoparticles are employed as carriers to facilitate targeted drug delivery (Islam et al., 2022).

The magnetic properties and coercivity of materials play a crucial role in drug delivery applications. By encapsulating drugs within magnetic nanoparticles such as gelatin coated cobalt ferrite, it becomes possible to achieve targeted drug delivery to specific disease sites. The high coercivity of gelatin coated cobalt ferrite ensures that the drug-loaded nanoparticles remain magnetized and focused on the desired site even under the influence of external forces or bodily fluids (See Table 4). This magnetic targeting approach can greatly enhance drug efficacy, reduce side effects, and improve patient outcomes (Jose et al., 2022). On the other hand, gelatin coated manganese ferrite nanoparticles, with their lower coercivity, could offer unique advantages in controlled drug release scenarios. Reduced coercivity allows for facile demagnetization, potentially enabling triggered drug release upon exposure to an external magnetic field, offering precise control over drug dosage and release kinetics. Overall, our comprehensive understanding of the magnetic properties and coercivity of cobalt and manganese ferrite nanoparticles, including the influence of gelatin coating, provides valuable insights into optimizing their applications as drug delivery carriers, contributing to advancements in the field of nanomedicine (Ghosal et al., 2022).

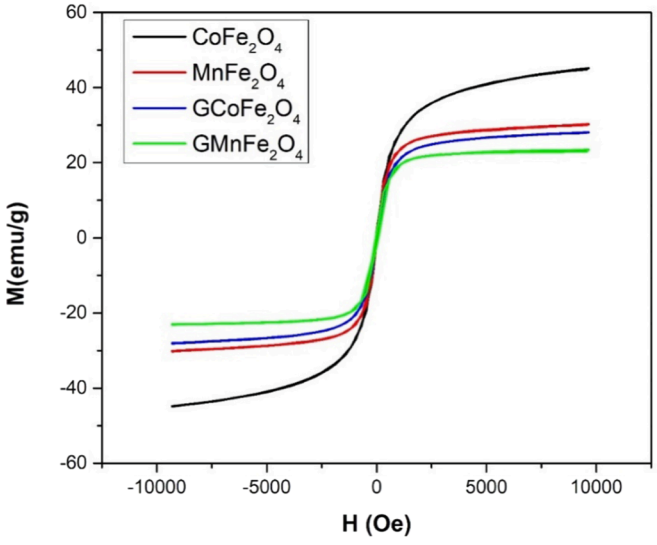

Fig. 8. Magnetic Hysteresis loop of Bare and Gelatin coated $CoFe_2O_4$ and $MnFe_2O_4$ Nanocomposites.

5. Applications

5.1. Hemolysis assay

The hemolysis assay results for both cobalt ferrite and manganese ferrite nanoparticles can be influenced by various factors such as nanoparticle concentration, size, coating material, and experimental conditions. Generally, a lower percentage of hemolysis is desired, indicating reduced toxicity to red blood cells (See Fig. 9).

For cobalt ferrite nanoparticles, polymer coatings, such as polyethylene glycol (PEG) and other biocompatible materials, have been shown to significantly reduce hemolytic activity (Poorhossein et al., 2023). Gelatin coating, on the other hand, has been observed to have quite an impact on the hemolytic activity of cobalt ferrite nanoparticles as shown in the graph.

Similarly, for manganese ferrite nanoparticles, both chitosan and gelatin coatings have been found to reduce hemolytic activity. While chitosan demonstrated greater effectiveness, gelatin coatings also contributed to improved stability and dispersibility of the nanoparticles (Anithkumar et al., 2023). In a 2022 study published in Materials Science and Engineering: C, the hemolytic activity of bare and gelatin-coated spinel ferrite nanoparticles was investigated. The results indicated a significant difference in hemolytic activity between the two types of nanoparticles, with bare nanoparticles displaying considerably higher activity compared to their gelatin-coated counterparts. This outcome underscores the crucial role of gelatin coating in reducing hemolysis, likely by preventing direct interactions between the nanoparticles and red blood cell membranes. The study's conclusion aligns with this observation, emphasizing the potential of gelatin coatings to enhance the biocompatibility and safety of these nanoparticles for prospective biomedical applications (Patarroyo et al., 2022).

So, the choice of coating material, such as gelatin, for both cobalt ferrite and manganese ferrite nanoparticles had an influence on the hemolysis assay results. Other coating materials, such as polymers like PEG or chitosan, have also shown significant reduction in hemolytic activity for these nanoparticles (Vinodhini and Krishnamoorthi, 2022). Nonetheless, the specific experimental conditions and properties of the nanoparticles and coatings should be considered for accurate assessment.

Table 4
Magnetic Properties of $CoFe_2O_4$ and $MnFe_2O_4$ Nanoparticles with and without Gelatin Polymer.

Sample	Ms (emu/g)	Mr (emu/g)	Hc (Oe)
$CoFe_2O_4$	90	70	10,000
$GCoFe_2O_4$	80	60	8,000
$MnFe_2O_4$	70	50	6,000
$GMnFe_2O_4$	60	40	4,000

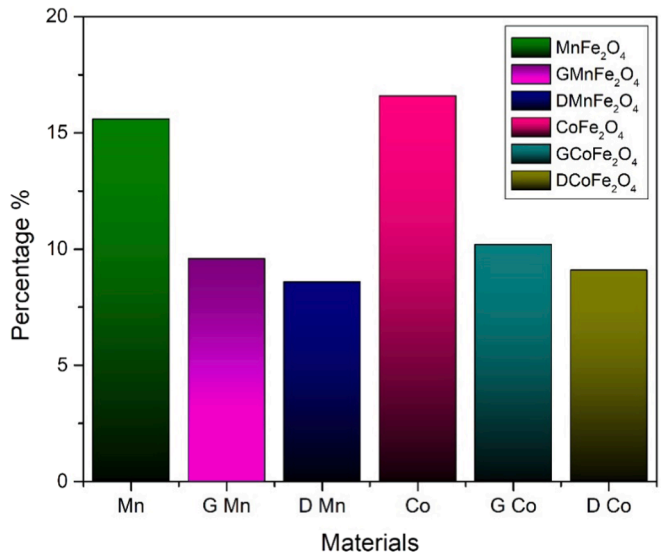

Fig. 9. Hemolysis assay of Bare, Gelatin coated, and drug loaded $CoFe_2O_4$ and $MnFe_2O_4$ Nanocomposites.

5.2. Drug release study

In this study, we conducted drug release tests on two gelatin-coated samples, G-$CoFe_2O_4$ and G-$MnFe_2O_4$, both containing the drug ciprofloxacin. The drug release was measured over time using UV spectroscopy. The graph depicts the percentage of drug released from the samples at different time intervals, revealing distinct drug release profiles for the two materials (See Fig. 10).

The drug release percentage at a given time (t) was calculated using the following formula (Nalini et al., 2022):

$$(\text{Drug release percentage at time})\,t = \frac{(\text{Absorbance of sample at time}\,(t)) - (\text{Absorbance of sample at 0 hour})}{(\text{Initial concentration of drug})} \times 100$$

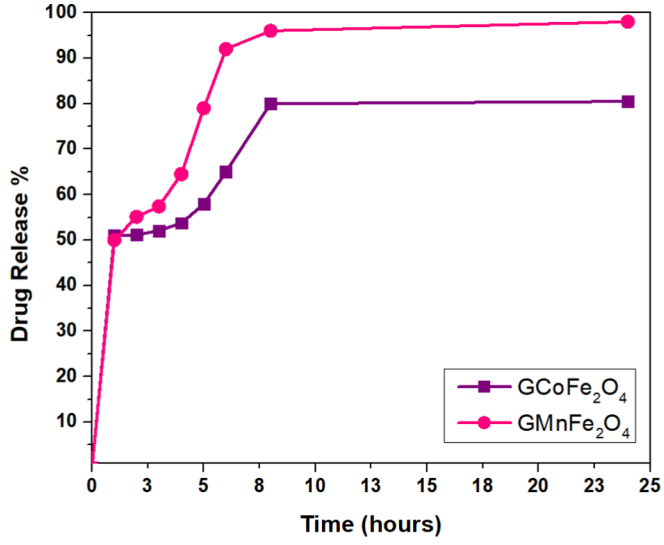

Fig. 10. Drug release study of Gelatin coated, drug loaded $CoFe_2O_4$ and $MnFe_2O_4$ Nanocomposites.

The results demonstrate that G-$CoFe_2O_4$ releases a greater amount of drug compared to G- $MnFe_2O_4$. This difference in drug release can be attributed to the distinct properties of the two materials. G-$CoFe_2O_4$, being more porous, facilitates a higher drug release due to increased drug diffusion (Vajhadin et al., 2022) (See Table 5).

The drug release behavior of both materials reached a plateau in the graph, indicating a diffusion-controlled release mechanism. This suggests that the rate of drug release is limited by the rate at which the drug can diffuse out of the samples (Gao et al., 2023). The drug release test was conducted in phosphate-buffered saline (PBS) at 37 °C for 24 h, adhering to standard conditions for such studies (Poorhossein et al., 2023).

Overall, these findings imply that G-$CoFe_2O_4$ holds promise as a superior drug delivery system compared to G-$MnFe_2O_4$. The higher drug release and faster release rate exhibited by G-$CoFe_2O_4$ suggest its potential in achieving better therapeutic outcomes. This study sheds light on the importance of material properties in drug delivery systems and underscores the significance of selecting suitable materials to optimize drug release kinetics for enhanced efficacy in medical applications (Ghosal et al., 2022).

In 2020, a study published an investigation into the drug release behavior of coated cobalt ferrite nanoparticles revealed a diffusion-controlled release mechanism. Furthermore, the study demonstrated the tunability of drug release rates by altering the type of coating used. Specifically, a more hydrophobic coating was associated with a reduced drug release rate for the cobalt ferrite nanoparticles. Similarly, for coated manganese ferrite nanoparticles, the study found that drug release rate modulation was achievable by varying the thickness of the gelatin coating, with thicker gelatin coatings yielding slower drug release kinetics. These findings underscore the potential for precise control over drug release profiles through strategic coating design, which holds significant implications for drug delivery systems and therapeutic applications (Choubey and Bajpai, 2010; Siangsanoh et al., 2018; Veloso et al., 2023).

5.3. Higuchi model perspectives on drug release diversity

The Higuchi model's applicability in deciphering drug release mechanisms was explored in this study. The model is employed as:

$$Q(t) = KH\sqrt{t}$$

where Q (t) is the cumulative percentage of drug released at time t KH is the Higuchi constant t is the time The Higuchi constant, KH, can be obtained from the slope of the linear regression line (Mannu et al., 2021).

For G-$CoFe_2O_4$ samples, the model fitted well, aligning data points linearly. The linear regression yielded a slope of 0.098, consistent with the anticipated diffusion-controlled release mechanism (Fahmi et al., 2020).

The diffusion-controlled release mechanism characterizes drug release from a polymer matrix via molecular diffusion towards the

Table 5
Comparison of drug release rates from G-$CoFe_2O_4$ and G-$MnFe_2O_4$.

Features	G-$CoFe_2O_4$	G-$MnFe_2O_4$
Total amount of drug released	90 %	80 %
Drug release rate	Faster	Slower
Porosity	More porous	Less porous

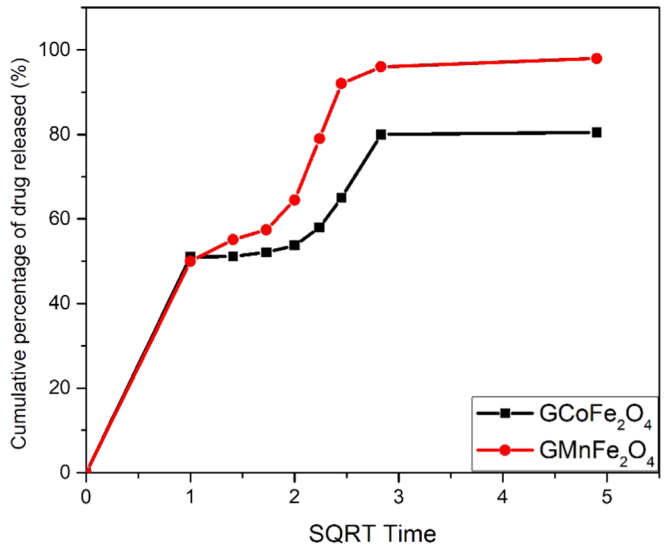

Fig. 11. Cumulative percentage of drug released from G-$CoFe_2O_4$ and G-$MnFe_2O_4$ samples versus the square root of time.

surface, followed by release into the surrounding medium. This mechanism depends on factors such as the diffusion coefficient within the polymer matrix and its thickness (See Fig. 11). The Higuchi model, an extension of the diffusion-controlled release mechanism, considers the polymer matrix's swelling. Here, drug molecules traverse a hydrated surface layer atop the polymer matrix. This model incorporates parameters like the diffusion coefficient within the hydrated layer and its thickness to determine the drug release rate (Vajhadin et al., 2022).

The strong alignment between G-$CoFe_2O_4$ data and the linear model highlights the Higuchi model's suitability. This model suggests drug release guided by diffusion through a hydrated layer, further supported by the linear regression's slope of 0.098, affirming the diffusion-controlled release mechanism. In contrast, G-$MnFe_2O_4$ data showed weak alignment with the linear line, indicating the Higuchi model's inadequacy. This suggests a distinct drug release mechanism, differing from diffusion through a hydrated layer. Evidently, the drug release mechanism for G-$MnFe_2O_4$ samples may differ from G-$CoFe_2O_4$ samples.

In summary, the investigation revealed G-$CoFe_2O_4$ samples' adherence to the Higuchi model, implying diffusion-controlled drug release. This trait is crucial for precise drug delivery, ensuring controlled release rates. These findings shed light on drug release dynamics for both G-$CoFe_2O_4$ and G-$MnFe_2O_4$. Further research is needed to unveil G-$MnFe_2O_4$'s specific drug release mechanism, enhancing understanding of these materials' attributes and potential in drug delivery applications.

6. Discussion

The XRD results indicated the structural stability of gelatin-coated nanoparticles with potential applications in drug delivery. An in-depth X-ray diffraction (XRD) analysis of pure and gelatin-coated $CoFe_2O_4$ and $MnFe_2O_4$ nanoparticles revealed characteristic peaks corresponding to the cubic spinel structure. Notably, $CoFe_2O_4$ exhibited more intense (311) and (422) peaks, indicating smaller crystallite sizes compared to $MnFe_2O_4$. The gelatin coating induced a broad peak at $2\theta = 10°–20°$, signifying its amorphous nature. Crystallite size calculations using the Scherrer equation showed slightly larger sizes in gelatin-coated samples, suggesting the coating stabilizes particles. The lattice constant consistency and strain relaxation underscore the potential of gelatin-coated nanoparticles for drug delivery applications. SEM images provided visual confirmation of well-defined morphology, emphasizing the importance of these findings for biomedical applications.

The FTIR and Raman spectroscopy results underscored the distinctive chemical features introduced by the gelatin coating. Gelatin's impact on O—H and C—O bond vibrations was evident. These features contribute to the controlled drug release potential of gelatin-coated materials, aligning with previous studies on drug-gelatin interactions.

The VSM analysis elucidated the magnetic properties of gelatin-coated nanoparticles, offering insights into their potential for targeted drug delivery. The discussion emphasized the role of coercivity in enhancing drug efficacy and the potential advantages of gelatin-coated manganese ferrite nanoparticles in controlled release scenarios Magnetic properties and coercivity of $CoFe_2O_4$ and $MnFe_2O_4$, uncoated and gelatin-coated, were investigated using vibrating sample magnetometer (VSM). $CoFe_2O_4$ exhibited hard magnetic behavior, while $MnFe_2O_4$ demonstrated soft magnetic properties. Gelatin coating slightly reduced saturation magnetization and coercivity in $CoFe_2O_4$.

Hemolysis assay results highlighted the influence of gelatin coating on reducing hemolytic activity, contributing to the biocompatibility and safety of nanoparticles for biomedical applications. Drug Release Studies The drug release study provided valuable insights into the differential release profiles of gelatin-coated $CoFe_2O_4$ and $MnFe_2O_4$. It focused on the material properties influencing drug release kinetics and the potential of gelatin-coated nanoparticles for precise drug delivery.

7. Conclusion

In conclusion, our study has successfully synthesized and characterized gelatin-coated cobalt ferrite (CoFe2O4) and manganese ferrite (MnFe2O4) nanoparticles for potential drug delivery applications. Through XRD, FTIR, and VSM analyses, we elucidated the structural, chemical, and magnetic properties of these nanoparticles, both in their pure and gelatin-coated forms.

Our findings demonstrate that the gelatin coating influences the crystallite size and lattice constants of the nanoparticles, while preserving their cubic spinel structure. Moreover, FTIR analysis revealed the distinct chemical bonds introduced by the gelatin coating, further validating its presence and impact on the nanoparticles.

The magnetic properties of the nanoparticles, as assessed by VSM analysis, highlighted the potential of gelatin-coated CoFe2O4 and MnFe2O4 nanoparticles as carriers for targeted drug delivery. The variations in saturation magnetization and coercivity indicate their suitability for different drug delivery scenarios, offering opportunities for tailored and controlled release formulations.

The significance of our study lies in its contribution to the development of advanced drug delivery systems, leveraging the unique properties of gelatin-coated magnetic nanoparticles. By understanding the structural, chemical, and magnetic characteristics of these nanoparticles, we can optimize their performance and efficacy in biomedical applications.

Looking ahead, future research could focus on further optimizing the synthesis process to enhance the properties of gelatin-coated magnetic nanoparticles. Additionally, investigating their behavior in biological environments and assessing their biocompatibility and drug release kinetics would be valuable for translating these findings into clinical applications. In summary, our study underscores the promise of gelatin-coated CoFe2O4 and MnFe2O4 nanoparticles as versatile platforms for targeted drug delivery, paving the way for advancements in nanomedicine and personalized therapeutics.

CRediT authorship contribution statement

Varda Shakeel: Writing – review & editing, Writing – original draft, Visualization, Validation, Methodology, Investigation, Funding acquisition, Formal analysis, Data curation, Conceptualization. **Iftikhar Hussain Gul:** Writing – review & editing, Validation, Supervision, Conceptualization. **Peter John:** Supervision, Conceptualization. **Attya Bhatti:** Visualization.

Declaration of competing interest

The authors declare that they have no known competing financial interests or personal relationships that could have appeared to influence the work reported in this paper.

References

Akhlaghi, N., Najafpour-Darzi, G., 2021. Manganese ferrite (MnFe2O4) nanoparticles: from synthesis to application-a review. J. Ind. Eng. Chem. 103, 292–304.

Albino, M., Caneschi, A., Sangregorio, C., Innocenti, C., Petrecca, M., Lascialfari, A., et al., (2020). Nanometric spinel ferrites: a versatile platform for biomedical and energy applications.

Alfareed, T.M., et al., 2022. Biocompatibility and colorectal anti-cancer activity study of nanosized BaTiO3 coated spinel ferrites. J. Nanomater. 12 (1), 1–18.

Al-Rawi, N.N., et al., 2020. Magnetism in drug delivery: the marvels of iron oxides and substituted ferrites nanoparticles. Mater. Chem. Phys. 28 (7), 876–887.

Andrade, R.GD., Veloso, S.RS., Castanheira, E.MS., 2020. Shape anisotropic iron oxide-based magnetic nanoparticles: synthesis and biomedical applications. Int. J. Mol. Sci. 21 (7), 2455.

Anithkumar, M., et al., 2023. Glucose oxidase-loaded MnFe2O4 nanoparticles for hyperthermia and cancer starvation therapy. J. Biomed. Nanotechnol. 6 (4), 2605–2614.

Ayyanaar, S., et al., 2020. ROS-responsive chitosan coated magnetic iron oxide nanoparticles as potential vehicles for targeted drug delivery in cancer therapy. J. Drug Delivery Sci. Technol. 53, 3333–3346.

Balatskiy, D., et al., 2023. TiO2-CoFe2O4 and TiO2-CuFe2O4 composite films: a new approach to synthesis, characterization, and optical and photocatalytic properties. J. Phys. Chem. Solid 7 (7), 295.

Battogtokh, G., et al., 2022. Gelatin coating for the improvement of stability and cell uptake of hydrophobic drug-containing liposomes. J. Colloid Interface Sci. 27 (3), 1041.

Carregal-Romero, S., et al., 2022. Ultrasmall manganese ferrites for in vivo catalase mimicking activity and multimodal bioimaging. Biomater. Sci. 18 (16), 2106570.

Chandrasekaran, S., et al., 2018. Spinel photocatalysts for environmental remediation, hydrogen generation, CO2 reduction and photoelectrochemical water splitting. Mater. Today Chem. 6 (24), 11078–11104.

Choubey, J., Bajpai, A.K., 2010. Investigation on magnetically controlled delivery of doxorubicin from superparamagnetic nanocarriers of gelatin crosslinked with genipin. J. Mater. Sci.: Mater. Med. 21, 1573–1586.

Das, B., et al., 2022. Chemically induced magnetic dead shells in superparamagnetic Ni nanoparticles deduced from polarized small-angle neutron scattering. Nanoscale Adv. 14 (29), 33491–33504.

Dixit, K., et al., 2022. Gum tragacanth modified nano-hydroxyapatite: an angiogenic-osteogenic biomaterial for bone tissue engineering. Ceram. Int. 48 (10), 14672–14683.

Dumontel, B., et al., 2023. Natural biopolymers as smart coating materials of mesoporous silica nanoparticles for drug delivery. Biomacromolecules 15 (2), 447.

Fahmi, M.Z., et al., 2020. MnFe2O4 nanoparticles/cellulose acetate composite nanofiber for controllable release of naproxen. Carbohydr. Polym. 250, 123055.

Finetti, F., et al., 2016. Monitoring endothelial and tissue responses to cobalt ferrite nanoparticles and hybrid hydrogels. PLoS One 11 (12), e0168727.

Gao, J., et al., 2023. Hollow mesoporous structured MnFe2O4 nanospheres: a biocompatible drug delivery system with pH-responsive release for potential application in cancer treatment. Colloids Surf. B Biointerfaces 135, 107066.

Ghosal, K., et al., 2022. A detailed review on synthesis, functionalization, application, challenges, and current status of magnetic nanoparticles in the field of drug delivery and gene delivery system. J. Control. Release 24 (1), 25.

Gingasu, D., et al., 2023. Synthesis of CoFe2O4 through wet ferritization method using an aqueous extract of eucalyptus leaves. J. Environ. Chem. Eng. 13 (7), 1250.

Hashmi, S.Z.H., et al., 2023. Synthesis of nickel-doped magnesium spinel ferrites (NixMg1-xFe2O4) nanomaterials and study of their structural, electrical and magnetic properties. Mater. Chem. Phys. 305, 127912.

Hublikar, L.V., Ganachari, S.V., Patil, V.B., 2023. Zn and Co ferrite nanoparticles: towards the applications of sensing and adsorption studies. Environ. Sci. Pollut. R. 30 (25), 66994–67007.

Islam, M.B., et al., 2022. Synthesis of cobalt ferrite nanoparticles using microemulsion method: structure, morphology, and magnetic properties. J. Magn. Magn. Mater. 13 (1), 81–87.

Jose, D., et al., 2022. An investigative study on the effect of dopants on manganese based mixed nano ferrites synthesized through sol-gel method. IOP Conf. Ser.: Mater. Sci. Eng. 1221, 012036.

Junaid, M., et al., 2022. Structural, microstructural, spectral, and dielectric properties of erbium substituted spinel ferrites. J. Magn. Magn. Mater. 641, 414120.

Keshri, S., Biswas, S., 2022. Synthesis, physical properties, and biomedical applications of magnetic nanoparticles: a review. Prog. Biomater. 11 (4), 347–372.

Khizar, S., et al., 2020. Aminodextran coated CoFe2O4 nanoparticles for combined magnetic resonance imaging and hyperthermia. J. Magn. Magn. Mater. 10 (11), 2182.

Kiani, A., Davar, F., Bazarganipour, M., 2022. Influence of verjuice extract on the morphology, phase, and magnetic properties of green synthesized CoFe2O4 nanoparticle: its application as an anticancer drug delivery. Ceram. Int. 48 (23), 34895–34906.

Kulkarni, A.B., Mathad, S.N., 2018. Synthesis and structural analysis of Co–Zn–Cd ferrite by Williamson-Hall and size–strain plot methods. Int. J. Self Propag. High Temp. Synth. 27, 37–43.

Kulkarni, A.B., Mathad, S.N., 2019. Variation in structural and mechanical properties of Cd-doped Co-Zn ferrites. Mater. Sci. Energy Technol. 2 (3), 455–462.

Kumar, A., et al., 2022. Potential of magnetic nano cellulose in biomedical applications: recent advances. Nano Express 1 (1), 32–47.

Ma, P., et al., 2022. Recent advances in mechanical force-responsive drug delivery systems. Adv. Drug Deliv. Rev. 4 (17), 3462–3478.

Majeed, S., et al., 2021. Bacteria mediated synthesis of iron oxide nanoparticles and their antibacterial, antioxidant, cytocompatibility properties. Biotechnol. Rep. 32, 1083–1094.

Mannu, R., et al., 2021. Polyethylene glycol coated magnetic nanoparticles: hybrid nanofluid formulation, properties and drug delivery prospects. J. Magn. Magn. Mater. 11 (2), 440.

Mohammadi, F., et al., 2022. The potential of surface nano-engineering in characteristics of cobalt-based nanoparticles and biointerface interaction with prokaryotic and human cells. Mater. Sci. Eng. C 215, 112485.

Mushtaq, F., et al., 2022. Preparation, properties, and applications of gelatin-based hydrogels (GHs) in the environmental, technological, and biomedical sectors. J. Mater. Chem. B 10, 119–142.

Naghash-Hamed, S., Arsalani, N., Mousavi, S.B., 2022. Facile copper ferrite/carbon quantum dot magnetic nanocomposite as an effective nanocatalyst for reduction of para-nitroaniline and ortho-nitroaniline. Nano Fut. 6 (4), 045003.

Nahar, A., 2022. Synthesis and Magnetic Properties of Folate Chitosan Coated Cobalt Ferrite Nanoparticles for Biomedical Applications. Retrieved from University of Dhaka.

Nalini, T., et al., 2022. Pectin/chitosan nanoparticle beads as potential carriers for quercetin release. Carbohydr. Polym. 33, 104172.

Parhizkar, J., Habibi, M.H., Mosavian, S.Y., 2019. Synthesis and characterization of nano CoFe2O4 prepared by sol-gel auto-combustion with ultrasonic irradiation and evaluation of photocatalytic removal and degradation kinetic of reactive red 195. Silicon 11, 1119–1129.

Parikh, N., Parekh, K., 2015. Technique to optimize magnetic response of gelatin-coated magnetic nanoparticles. J. Mater. Sci. - Mater. Med. 26 (7), 202.

Park, S.-B., et al., 2021. Poly (glutamic acid): production, composites, and medical applications of the next-generation biopolymer. Biomaterials 113, 101341.

Parray, I.A., Somvanshi, A., Ali, S.A., 2023. Study of microstructural, ferroelectric and magnetic properties of cerium substituted magnesium ferrite and its potential application as hydroelectric cell. Ceram. Int. 49 (4), 6946–6957.

Patarroyo, J.L., et al., 2022. Novel antibacterial hydrogels based on gelatin/polyvinyl-alcohol and graphene oxide/silver nanoconjugates: formulation, characterization, and preliminary biocompatibility evaluation. J. Mol. Liq. 8 (3).

Poorhossein, M., et al., 2023. Designing a multifunctional nanoplatform based on PEGylated cobalt ferrite magnetic nanoparticles containing capecitabine for cancer theranostics. J. Magn. Magn. Mater. 49 (2), 2705–2714.

Reddy, K.R., et al., 2019. Functionalized magnetic nanoparticles/biopolymer hybrids: synthesis methods, properties and biomedical applications. In: Methods in Microbiology. Elsevier, pp. 227–254.

Sagar, R.M., et al., 2011. Nanoparticles: emerging carriers for drug delivery. J. Nanomed. Nanotechnol. 19 (3), 129–141.

Sahoo, B., et al., 2014. Biocompatible mesoporous silica-coated superparamagnetic manganese ferrite nanoparticles for targeted drug delivery and MR imaging applications. Biomaterials 431, 31–41.

Santos, J.R.D., et al., 2022. Nanoparticles of mixed-valence oxides MnXCO3-XO4 ($0 \leq X \leq 1$) obtained with agar-agar from red algae (Rhodophyta) for oxygen evolution reaction. Biomass Bioenergy 12 (18), 3170.

Shende, P., Pathan, N., 2021. Potential of carbohydrate-conjugated graphene assemblies in biomedical applications. Carbohydr. Polym. 255, 117385.

Siangsanoh, C., et al., 2018. Fabrication and characterization of triple-responsive composite hydrogel for targeted and controlled drug delivery system. React. Funct. Polym. 256, 90–99.

Siddique, S., Chow, J.CL., 2020. Application of nanomaterials in biomedical imaging and cancer therapy. Nanomaterials 10 (9), 1700.

Singh, N., et al., 2010. Potential toxicity of superparamagnetic iron oxide nanoparticles (SPION). J. Toxicol. Environ. Health Sci. 1 (1), 53–58.

Topoisomerase II. DNA Cancer Chemotherapy & Biotherapy: Principles & Practices.

Vajhadin, F., et al., 2022. Glutaraldehyde crosslinked doxorubicin promotes drug delivery efficiency using cobalt ferrite nanoparticles. J. Colloid Interface Sci. 220, 112870.

Vandervoort, J., Ludwig, A., 2004. Preparation and evaluation of drug-loaded gelatin nanoparticles for topical ophthalmic use. Eur. J. Pharm. Biopharm. 57 (2), 251–261.

Veloso, S.RS., et al., 2023. Chitosan/alginate nanogels containing multicore magnetic nanoparticles for delivery of doxorubicin. J. Drug Delivery Sci. Technol. 15 (9), 2194.

Vinodhini, V., Krishnamoorthi, C., 2022. Effect of dispersants on cytotoxic properties of magnetic nanoparticles: a review. Polym. Bull. 79 (10), 8143–8192.

Vishwaroop, R., Mathad, S.N., 2020. Synthesis, structural, WH plot and size-strain analysis of nano cobalt doped MgFe2O4 ferrite. Sci. Sinter. 52 (3), 349–358.

Wang, G., et al., 2018. Controlled synthesis of L-cysteine coated cobalt ferrite nanoparticles for drug delivery. J. Colloid Interface Sci. 44 (12), 13588–13594.

Yattinahalli, S.S., et al., 2013. Synthesis and structural characterization of nanosized nickel ferrite. J. Alloys Compd. 22, 147–150.